micro

MDPI

Article

The Design, Simulation, and Parametric Optimization of an RF MEMS Variable Capacitor with an S-Shaped Beam

Shakila Shaheen *, Tughrul Arslan and Peter Lomax

Scottish Microelectronics Centre, University of Edinburgh, Edinburgh EH9 3FF, UK; tughrul.arslan@ed.ac.uk (T.A.); peter.lomax@ed.ac.uk (P.L.)
* Correspondence: s.shaheen-2@sms.ed.ac.uk

Abstract: This study presents the design and simulation of an RF MEMS variable capacitor with a high tuning ratio and high linearity factor of capacitance–voltage response. An electrostatic torsion actuator with planar and non-planar structures is presented to obtain the high tuning ratio by avoiding the occurrence of pull-in point. In the proposed design, the capacitor plate is connected to the electrostatic actuators by using the s-shaped beam. The proposed design shows a 138% tuning ratio with the planar structure of the actuator and 167% tuning ratio by implementing the non-planar structure. A linearity factor of 99% is attained by adjusting the rates at which the capacitor plate rises as the actuation voltage increases and the rate at which the capacitance decreases as the plate rises. Parametric optimization of the design is performed by utilizing the finite element method (FEM) analysis and high-frequency structural simulator (HFSS) analysis to obtain an optimized high-tuning ratio RF MEMS varactor at low actuation voltage. S-parameters of the design are presented on HFSS, with a 50 ohm coplanar waveguide (CPW) serving as the transmission line. The proposed RF MEMS varactor can be utilized in tunable RF devices.

Keywords: RF MEMS; variable capacitor; FEM analysis; HFSS analysis; s-shaped beam; s-parameters; planar and non-planar actuators

Citation: Shaheen, S.; Arslan, T.; Lomax, P. The Design, Simulation, and Parametric Optimization of an RF MEMS Variable Capacitor with an S-Shaped Beam. *Micro* **2024**, *4*, 474–489. https://doi.org/10.3390/micro4030030

Academic Editors: Nicola Pio Belfiore, Vittorio Ferrari, Elisabetta Comini, Marco Baù and Dario Zappa

Received: 15 April 2024
Revised: 2 July 2024
Accepted: 18 July 2024
Published: 14 August 2024

1. Introduction

Microelectromechanical systems (MEMS) variable capacitors using parallel plates are becoming increasingly popular in radio frequency (RF) applications due to their high-quality factor, fast response time, and straightforward design. Reconfigurable RF front-end modules can be made easy by microelectromechanical system (MEMS) changeable capacitors, which can help them fulfill space limitations by requiring fewer components and meeting the requirements of modern multi-band applications. Moreover, MEMS components have reduced power consumption, greater quality factor, and lower insertion loss when compared to solid-state equivalents such as Schottky varactors and p-n junction diodes [1]. Applications for reconfiguring MEMS variable capacitors include tunable impedance matching or antenna frequency tuning to maximize antenna efficiency in various environments and reconfigurable filters to increase performance selectivity while requiring fewer components overall [2]. RF filters [3,4], phase-locked loop circuits (PLLs) [5], voltage-controlled oscillators (VCOs) [6], and other applications are based on MEMS varactors.

Parallel-plate MEMS variable capacitors, which are usually based on attractive electrostatic actuation, show a nonlinear capacitance-to-voltage (C-V) response despite their relatively high-quality factors [7,8]. Because capacitance is dependent on distance, a decrease in plate distance results in an increase in capacitance. The capacitance increases as the actuation voltage increases because the plate travels faster in the direction of the decreasing gap. Such nonlinearities can cause loop bandwidth changes in phase-locked loops (PLLs) and nonconstant phase noises in voltage-controlled oscillators (VCOs), according to several studies. [9].

Different actuation devices are used for actuation purposes in RF MEMS varactors. The most commonly used actuators are electrostatic actuators due to low power consumption and fast response time.

The pull-in point is an important parameter of the parallel plate RF MEMS varactor. After applying the voltage, an electrostatic force is produced. Due to the produced force, the top plate moves in a downward direction. When the top plate covers one-third of the distance, electrostatic force overcomes the mechanical force. This is the instability point of the parallel plate RF MEMS varactor at which the top plate snaps down and no capacitance tuning occurs after this point.

Several techniques, such as utilizing variable gap spacing variations and introducing nonlinear mechanical components, have been put forth to increase the linearity of MEMS varactors [10]. One more method, which is detailed in [11,12], utilizes a levering structure to change the electrostatic varactor's closing-gap motion into a rising gap movement [13], producing a capacitance–voltage connection that is more linear. However, this method shows pull-in limitations. A segmented plate linear capacitor with a noteworthy 99.7% LF was introduced in [14–18] but the tuning ratio was limited to 68% tuning ratio. A variable capacitor with a high C-V response and 50% tunability was presented in [19]. An optimized MEMS variable capacitor was proposed to obtain the high linear capacitance–voltage response; however, this method also shows pull-in limitations [20]. To preserve improved linearity, the C-V spring stiffening technique is used to increase the varactor's rigidity as the voltage approaches the pull-in point [21]. However, this method makes it challenging to determine the control voltage range and capacitance value. One of the techniques of torsion spring structure is utilized to obtain a high-capacitance tuning ratio and linear capacitance–voltage response, but it shows pull-in instability after one-third of the distance [22]. Recently one of the techniques with repulsive actuation was proposed with high linearity and tunability, but this method works within 1–100 volts, which is very high and needs to be addressed [23].

The tuning ratio of these variable capacitors was limited due to the pull-in point because the capacitance value of these capacitors changes dramatically when the actuation voltage approaches the pull-in point. In the literature, several attempts have been made to improve the linearity factor of capacitance–voltage response but the tuning ratio was limited due to pull-in instability. It was found difficult to obtain a high tuning ratio with high linearity due to pull-in instability. Some of the techniques made it possible to overcome the pull-in instability and nonlinear capacitance–voltage response, but these devices work at very high actuation voltage [23]. It was challenging to attain a significant capacitance tuning ratio with the high linear capacitance–voltage response. Therefore, during the past ten years, there has been a great deal of interest in the development of MEMS variable capacitors that offer both high linearity factor and a large capacitance tuning ratio.

To overcome these issues, this study proposed a novel design of an RF MEMS varactor with planar and non-planar structures of the electrostatic actuator to improve the performance of the RF MEMS variable capacitor. The proposed study presents several notable contributions to the research. One of the notable contributions is to avoid the risk of pull-in instability by implementing the non-planar structure of the electrostatic torsion actuator. This is the major limitation of the traditional MEMS varactor. Due to pull-in instability, the tuning ratio of the MEMS varactor is limited and affects the performance of the MEMS varactor. Another noteworthy contribution is to obtain the linear capacitance-voltage response by introducing the novel design of the RF MEMS varactor.

A novel linear RF MEMS varactor design is proposed to obtain a high capacitance tuning ratio and high linearity. An electrostatic actuator is used to connect the actuator part to the capacitor plate by utilizing an s-shaped beam. It is the first demonstration of the s-shaped beam to be used as a connecting link between two parts. Two modes of electrostatic actuators are discussed to obtain a high tuning ratio with high linearity. The proposed design requires low actuation voltage in the planar structure of the electrostatic actuator due to the low spring constant. Parametric optimization of the proposed design is performed by

utilizing ANSYS APDL analysis and high-frequency structural simulator (HFSS) analysis to obtain a high tuning ratio RF MEMS varactor with low actuation voltage. In the next part of the research paper, the RF MEMS varactor with an electrostatic actuator having a non-planar structure is implemented to obtain the linear RF MEMS varactor with high tuning ratio by avoiding the risk of instability.

2. Design Methodology

The traditional parallel MEMS varactor exhibits nonlinear behavior due to the rise in capacitance and decreases in the air gap between them when an actuation voltage is applied. The capacitance increases as the actuation voltage increases because the plate travels faster in the direction of the decreasing gap. Thus, a nonlinear capacitance–voltage response results from a more steeply increasing rate of capacitance increment with an increase in voltage. This is the drawback of the traditional parallel MEMS varactor.

There is a linear capacitance–voltage response in the proposed design. The capacitance reduces linearly with applied voltage while the distance between the plates extends as the voltage rises. The traditional decreasing-gap movement of the electrostatic actuator is changed into a rising-gap movement by utilizing an s-shaped beam, which allows for the capacitance to decrease as the actuation voltage increases. Linear response of capacitance–voltage is attained by adjusting the rates at which the capacitor plate rises as the actuation voltage increases and the rate at which the capacitance decreases as the plate rises. The linearity response of the conventional and proposed MEMS variable capacitor is shown in Figure 1.

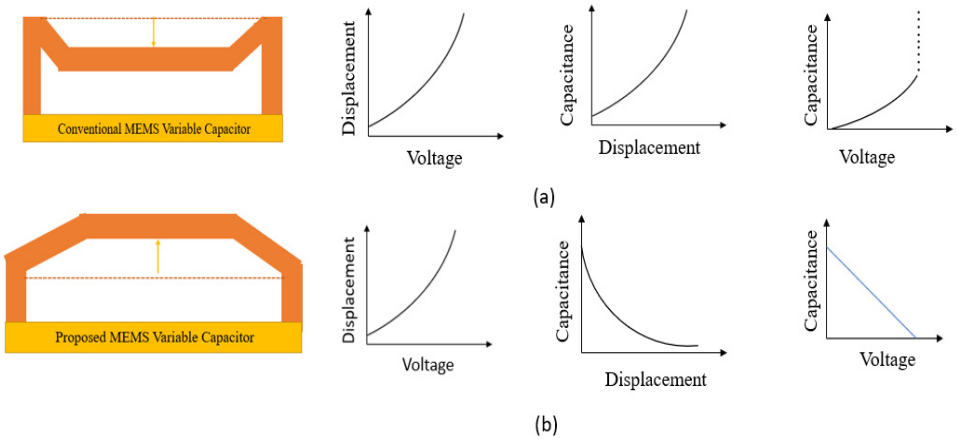

Figure 1. Schematic view of the (**a**) conventional MEMS variable capacitor and (**b**) proposed MEMS variable capacitor showing linear capacitance–voltage response.

In the proposed design, the actuator is utilized to move the capacitor plate in the rising direction linearly with applied voltage. An electrostatic torsion actuator is presented, which contains two torsion springs. An electrostatic torsion actuator with its planar and non-planar form is discussed in this design to obtain a high tuning ratio by avoiding the pull-in point.

The length of the upper electrode and bottom plate is a_1 and a_2, respectively, while w is the width of the electrode. A cross-sectional view of the electrostatic torsion actuator is shown in Figure 2b. For the planar mode of the electrostatic actuator, the length of the upper electrode is equal to the bottom plate; however, for the non-planar type of electrostatic actuator, unequal lengths of the top electrode and bottom plate are presented.

The proposed design is composed of two segments: the actuator part and the capacitor part. The electrostatic actuator is joined to the capacitor part by introducing the s-shaped beam. This is the first demonstration of an s-shaped beam to be utilized to connect the actuator part and capacitor part. The planned RF-MEMS variable capacitor is shown in Figure 2a.

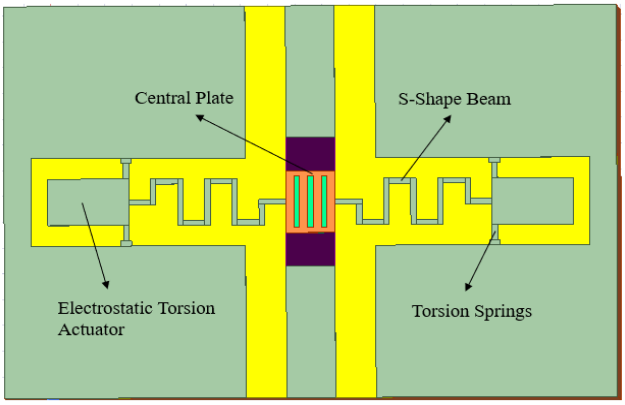

(**a**)

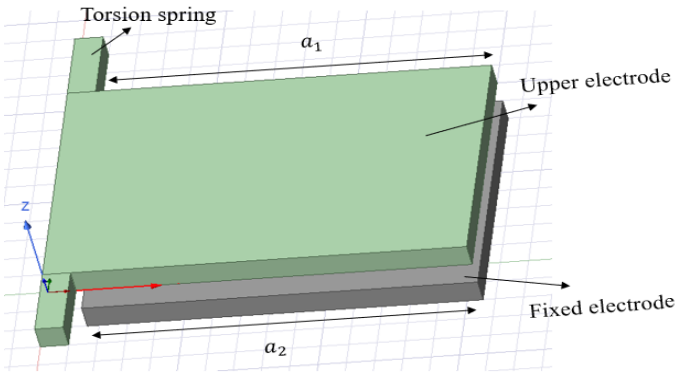

(**b**)

Figure 2. Schematic view of the (**a**) proposed RF MEMS variable capacitor and (**b**) electrostatic actuator.

After applying the voltage in the electrostatic actuator, electric force is formed between the plates causing the top plate to move. The s-shaped beam is employed here to drive the capacitor plate in the rising gap direction. So, the upstate capacitance will be minimal due to the rising movement of the capacitor plate. Consequently, the tuning ratio will be maximum. Figure 3a,b shows the simplified view of the RF MEMS variable capacitor before and after applying the voltage.

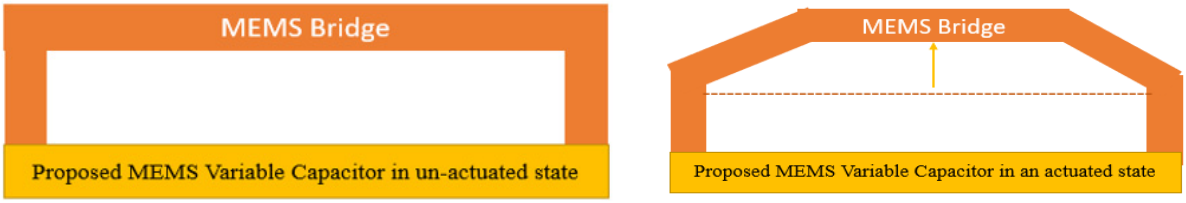

(**a**) (**b**)

Figure 3. (**a**) Simplified view of the RF MEMS variable capacitor in un-actuated condition (**b**) up state of the proposed RF MEMS varactor after applying the voltage.

The electrostatic torque is made in the actuator when voltage is applied across them. At equilibrium, electrostatic torque becomes equal to the mechanical torque [24].

$$E_T = M_T$$

$$\frac{\varepsilon w V^2}{2\alpha_{pull\ in}{}^2}\left[\frac{1}{1-\frac{a_{2\alpha_{pull\ in}}}{a_1\ \alpha_{max}}} - 1 + \ln\left(1-\frac{a_{2\alpha_{pull\ in}}}{a_1\ \alpha_{max}}\right)\right] = T_s\alpha_{pull\ in} \quad (1)$$

where T_s is the spring constant, w is the width of the plate in the actuator part, $\alpha_{pull\ in}$ is the pull-in angle, and α_{max} is the maximum pull-in angle.

By expanding the left side of Equation (1) into series form:

$$\frac{\left(\frac{a_2}{a_1\ \alpha_{max}}\alpha_{pull\ in}\right)^2}{2} + \frac{\left(\frac{a_2}{a_1\ \alpha_{max}}\alpha_{pull\ in}\right)^3}{3} = \frac{2}{\varepsilon w V^2} T_s {\alpha_{pull\ in}}^3 \quad (2)$$

The force becomes stronger with an increase in voltage. There will be a point when electrostatic force becomes strong enough to overcome the mechanical force, so plates come in contact with each other at this point. This is the instability between two positions and is called the pull-in point and can be described by using the following equation [24]:

$$V_{pull\ in} = \sqrt{\frac{9.68\ T_s\ {\alpha_{pull\ in}}^3}{\varepsilon w}} \quad (3)$$

There is a beam force in the s-shape beam due to which the central capacitor plate moves in the upward direction.

The rising movement of the capacitor plate can be expressed as follows:

$$d_1 = \alpha_{pull\ in} \times l_b \quad (4)$$

where l_b indicates the length of the s-shaped beam and $\alpha_{pull\ in}$ is the angle at the pull-in.

It is mainly dependent on the length of the s-shaped beam and the pull-in angle of the actuator plate. Capacitor plate displacement will be maximum for maximum downward travel of the actuator plate and having the higher pull-in angle.

Pull-in angle $\alpha_{pull\ in}$ can be derived from Equation (2):

$$\alpha_{pull\ in} = \frac{-3a_1{a_2}^2\alpha_{max} + \frac{12T_s(a_1\alpha_{max})^3}{\varepsilon w V^2}}{2{a_2}^3} \quad (5)$$

The capacitance of the proposed varactor at the initial position is shown as follows:

$$C_{down\ state} = \frac{\varepsilon A}{d} \quad (6)$$

where A is the area of the central plate, and the initial gap is represented by d.

As there is an increase in distance between the capacitor plates by d_1 by applying the voltage, the up capacitance can be calculated as follows:

$$C_{up\ state} = \frac{\varepsilon A}{d + d_1} \quad (7)$$

where d_1 is the increased gap between the plates after applying the voltage which can be shown from Equation (4).

The capacitance tuning ratio can be established as follows [25]:

$$C_r = \frac{C_{down\ state}}{C_{up\ state}} \quad (8)$$

For the RF MEMS variable capacitor to have the maximum tuning ratio, downstate capacitance should be maximum, and up-capacitance should be minimum. In the proposed design, minimum up capacitance is achieved by increasing the capacitor plate's height, which is desirable for a maximum tuning ratio.

3. Simulation Results with Planar Electrostatic Actuator

3.1. Mechanical Analysis of RF MEMS Variable Capacitor

Ansys APDL was used for the finite element method (FEM) analysis of the 3D model of the RF MEMS variable capacitor with the planar structure of the electrostatic actuator. Structural analysis was carried out with shell 63 elements on ANSYS APDL. Shell 63 has bending and membrane skills and has six degrees of freedom (DOF) on each node. Meshing is also an important parameter in ANSYS for the accuracy of the solution. Element edge length is considered 3 and the number of element divisions are considered 1 in the meshing of the structure.

Aluminum is utilized for bridge material. Primarily, there is a 3 µm gap between the plates. After exposure of voltage in the electrostatic actuator plates, the electric force is generated causing the top plate to move in the decreasing gap direction due to force. The s-shaped beam is utilized to increase the gap between the plates in the varactor part. There are slices in the capacitor plate to increase the area tunability of the varactor. Slices in the capacitor plate are also essential to avoid stiction issues and have the fast switching speed of the device. Figure 4 shows the dimensions of the planned RF MEMS variable capacitor.

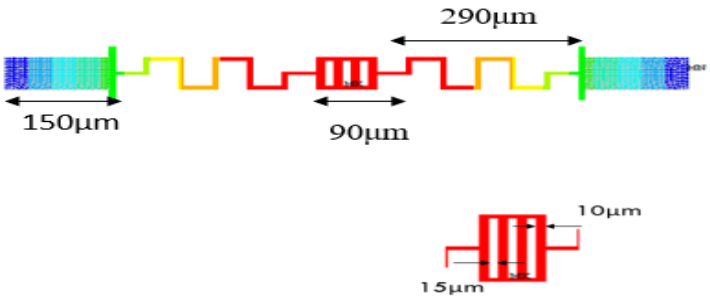

Figure 4. Top view of proposed RF MEMS variable capacitor.

The ANSYS findings are displayed in Figure 5, in which the movement of the actuator plate is shown in a downward position and the movement of the capacitor plate is shown in the opposite direction of the actuator plate. It demonstrates the actuator plate displacement of 1.16 µm in the downward direction, while the capacitor plate displacement of 1.14 um is shown in the increasing gap direction. The design parameters of the proposed RF MEMS varactor are listed in Table 1.

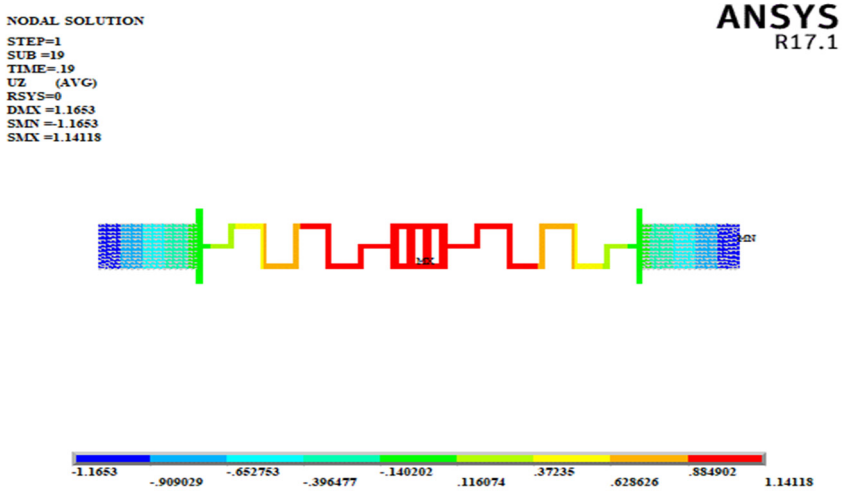

Figure 5. ANSYS results showing central plate displacement in the z-direction.

Table 1. Design parameters of RF MEMS variable capacitor.

Parameter	Values (um)
Air gap	3
Length of electrode	150
Substrate thickness	525
Transmission line dimensions	75/90/75
S-shaped beam length/width/thickness	290/90/1.8
Area of the central plate	90 × 90

Figure 6a,b displays the displacement of the capacitor plate and up capacitance respectively at different voltages. Based on Figure 6, the maximum central plate displacement of 1.14 um in the upward direction is achieved at 15.2 V.

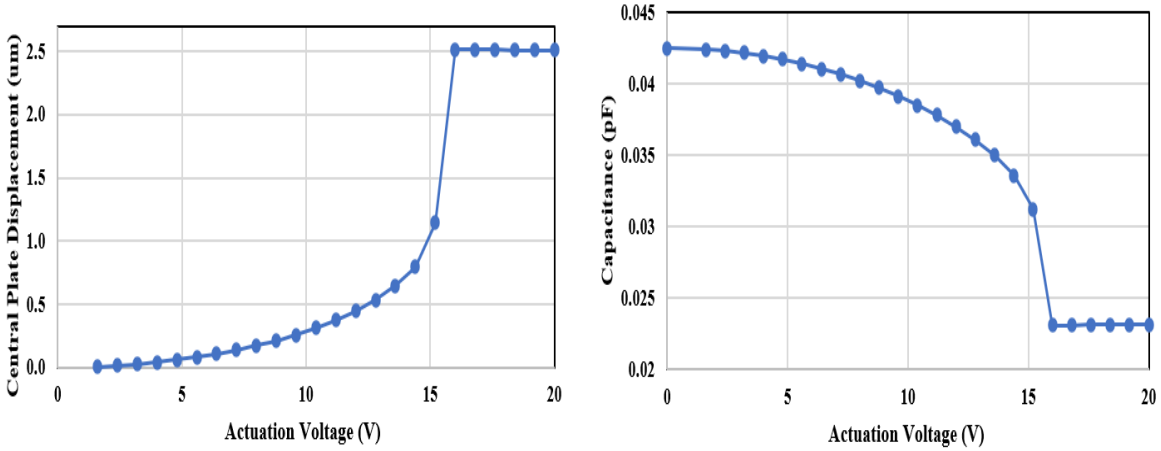

(**a**) (**b**)

Figure 6. Graphical view of (**a**) central plate displacement (**b**) capacitance.

When actuation voltage is supplied in the actuator portion, stress is produced on the structure, which is called von Mises stress. Von Mises stress was observed in ANSYS APDL and is shown in Figure 7. Maximum stress is shown on the torsion spring's end. The torsion spring's end pressure is 30.4 MPa, which guarantees that the structure can sustain the applied voltage without collapsing because it is less than the aluminum's yield strength.

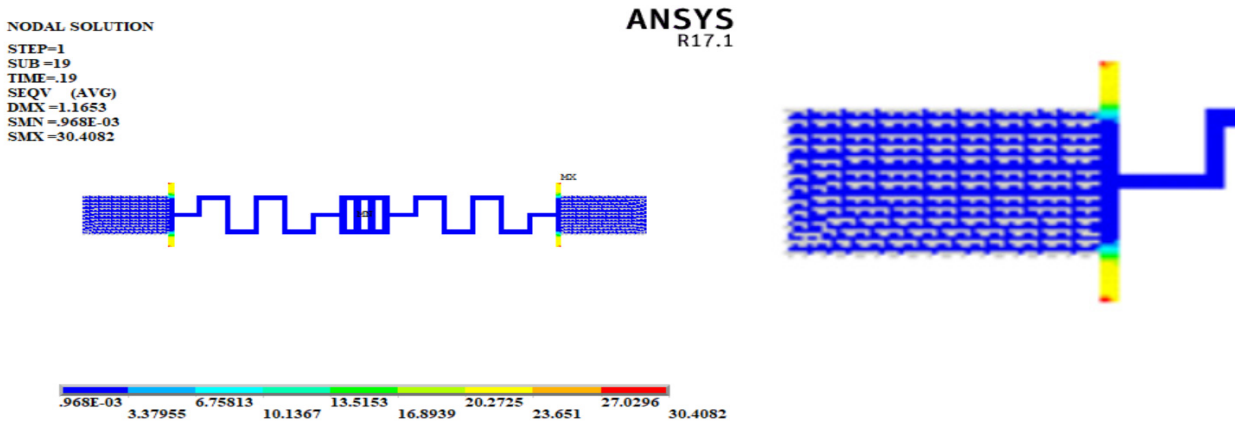

(**a**) (**b**)

Figure 7. (**a**) Von Mises stress analysis (**b**) showing maximum stress at the end of torsion springs.

3.2. Electrical Analysis of Proposed RF MEMS Variable Capacitor

Electrical analysis of the proposed RF MEMS variable capacitor was carried out in the student version of high-frequency structural simulator (HFSS) software. The coplanar waveguide (CPW) is used as a transmission line with two ground lines and a central signal line on the same plane. It is utilized with the characteristic impedance of 50 ohms to avoid return losses due to mismatching. The dimensions of the coplanar waveguide (CPW) are 75/90/75 µm. The length of the coplanar waveguide (CPW) is 760 µm. Aluminum is used as a center conductor. Figure 8 shows the full layout of the proposed RF MEMS variable capacitor.

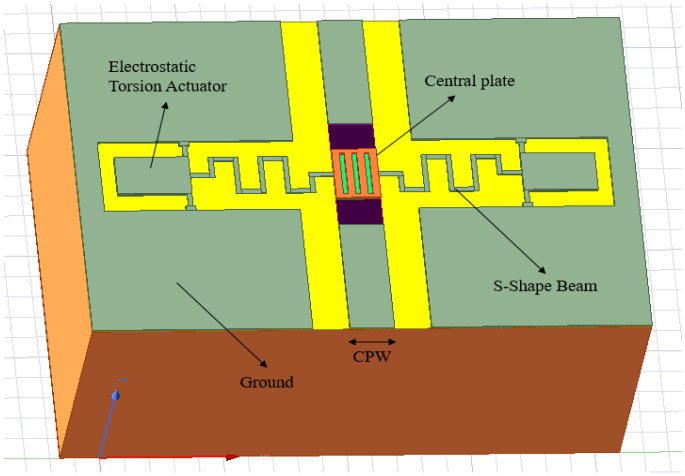

Figure 8. HFSS layout of the proposed RF MEMS variable capacitor.

The RF MEMS variable capacitor is designed for both ON and OFF states. For both actuated and un-actuated states, the RF MEMS varactor remains in the ON state. Scattering parameters are measured for both states. Return loss is represented as S11 and insertion loss is indicated as S21.

When there is no gap between the plates in the capacitor part, scattering parameters show the off-state properties of the structure. Maximum isolation and 0 dB return loss are the optimal conditions for the OFF state [1]. The scattering parameters in the OFF state for the 1–10 GHz frequency range are shown in Figure 9a,b. At 5.3 GHz, Figure 9b depicts the peak isolation of −31.81 dB. At this frequency, the return loss in the OFF state is −0.26 dB. Thus, at 5.3 GHz, the device yields the best results.

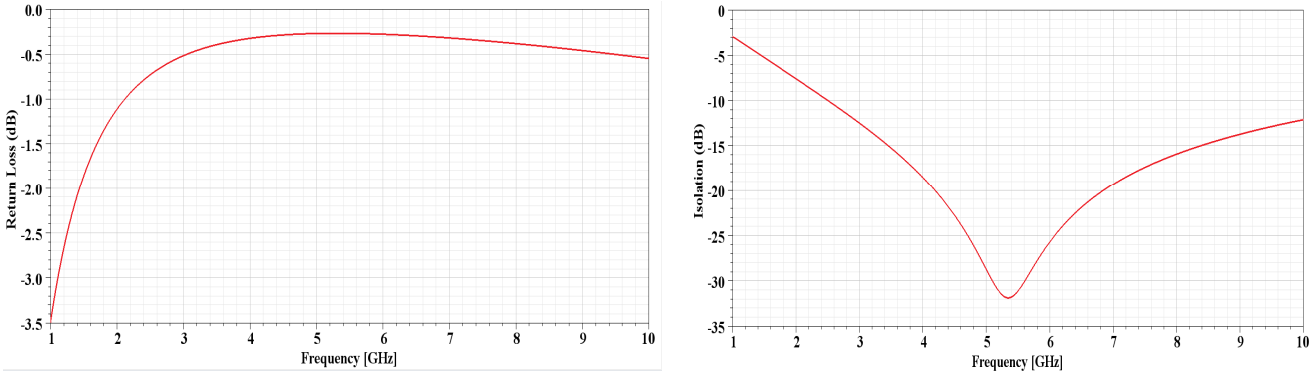

(**a**) (**b**)

Figure 9. Scattering parameters of RF-MEMS variable capacitor in OFF state: (**a**) return loss; (**b**) insertion loss.

The RF MEMS variable capacitor is in its initial state when there is no actuation voltage. Figure 10 displays the scattering parameters of the proposed RF MEMS varactor in an un-actuated state. Return loss fluctuates between −49.25 dB and −34.10 dB over the frequency range of 1–10 GHz, while the insertion loss varies between −0.0181 dB and −0.047 dB. As the proposed RF MEMS varactor performed well at 5.3 GHz, the return loss and insertion loss at 5.3 GHz were −38.61 dB and −0.033 dB, respectively.

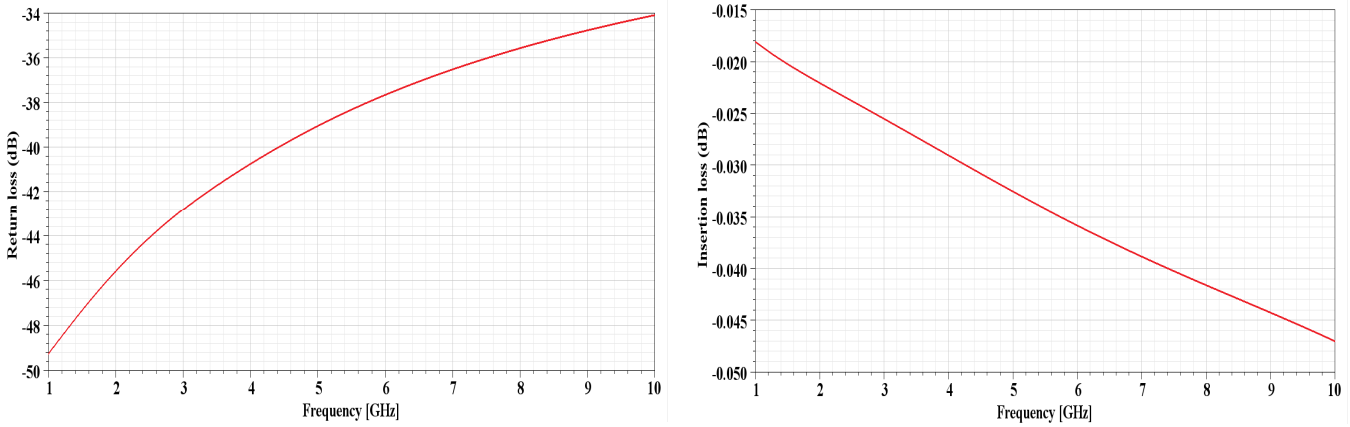

(**a**) (**b**)

Figure 10. RF-MEMS variable capacitor in un-actuated condition: (**a**) return loss; (**b**) insertion loss.

Figure 11 illustrates the scattering parameters of the RF MEMS variable capacitor after the actuation of voltage. In this instance, the gap is raised because voltage causes the capacitor top plate to move in the direction of the rising gap. The capacitor plate travels 1.14 um in the direction of the growing gap. Return loss fluctuates between −37.94 dB and −27.80 dB in the 1–10 GHz frequency band, while the insertion loss changes its values between −0.018 dB and −0.048 dB. The optimum operating frequency of the RF-MEMS variable capacitor is 5.3 GHz. Thus, at this frequency, the insertion loss is −0.0336 dB and the return loss is −32.02 dB, which can be shown in Figure 11.

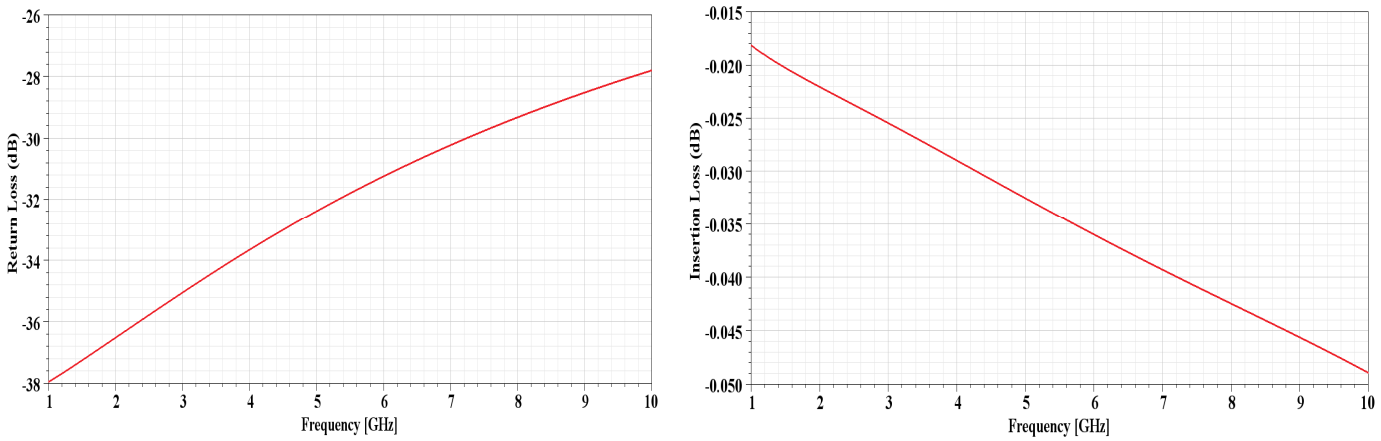

(**a**) (**b**)

Figure 11. RF-MEMS variable capacitor in actuated condition: (**a**) return loss; (**b**) insertion loss.

3.3. Parametric Optimization of Proposed RF MEMS Variable Capacitor

Parametric optimization of the proposed design is carried out to obtain a high tuning ratio RF MEMS varactor at low actuation voltage. Parametric analysis is performed to evaluate the performance of the RF MEMS variable capacitor. When the varactor is being fabricated, a parametric investigation of the device is required to study the impact of changing various parameters for long-term reliability.

The RF MEMS varactor was optimized to verify its performance within a given range of dimensions (width, gap, and length). These dimensions of width, length, and gap have a major impact on the performance of the RF MEMS variable capacitor. By changing the values of these parameters within a frequency range of 1–10 GHz, the performance of the RF MEMS variable capacitor was examined to optimize these parameters. Figure 12 shows the parametric optimization approach of the proposed design.

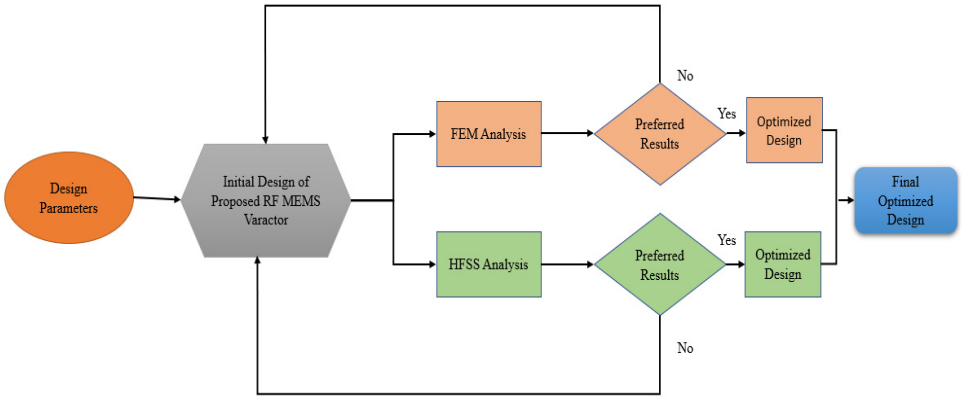

Figure 12. Parametric optimization approach for proposed RF MEMS variable capacitor.

3.3.1. Optimizing the Contact Area

The central plate contact area is optimized to obtain a high capacitance tuning ratio. Table 2 shows the tuning ratio of the RF MEMS variable capacitor with different central plate areas based on the ANSYS results. It shows the upstate and downstate capacitance of the proposed RF MEMS variable capacitor for different central plate areas. Maximum displacement of the capacitor plate in the upward direction is achieved for design 1 with a 90 × 90 central plate area. Consequently, there will be a high tuning ratio in this case. Table 2 shows the comparison of the RF MEMS variable capacitor in terms of the tuning ratio for different contact areas.

Table 2. Comparison of different contact area RF MEMS variable capacitor.

Design	**1**	**2**	**3**
Area (um)	90 × 90	90 × 120	90 × 160
Cdown (fF)	23.906	31.874	42.5
Cup (fF)	17.3	23.4	31.2
Tuning ratio (%)	138	136	136

3.3.2. Electrode Length Optimization

Figure 13 shows the central plate displacement and capacitance at different electrode lengths. Better performance is obtained for an electrode length of 150 µm in terms of tuning ratio at low actuation voltage. However, a greater capacitor plate displacement is obtained for an electrode length of 90 um as compared to 150 um. The purpose is to obtain a high tuning ratio MEMS variable capacitor at low actuation voltage, so 150 um is considered for the proposed MEMS variable capacitor.

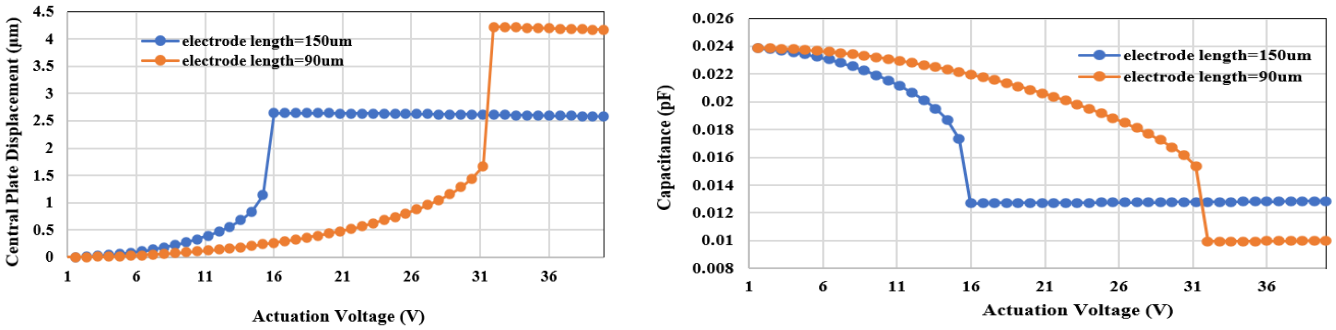

(**a**) (**b**)

Figure 13. Comparison of (**a**) central plate displacement at different electrode lengths and (**b**) up-capacitance at different electrode lengths.

3.3.3. S-Shaped Beam Length Optimization

Parametric analysis is done to get the optimized s-shaped beam length. Figure 14a,b shows the ANSYS results for 290 um and 190 um s-shaped beam lengths. The capacitor plate displacement of the MEMS variable capacitor with 290 um is 1.14 um; however, for the MEMS varactor with 190 um, it is 0.60 um. Maximum displacement is achieved for 290 um s-shape beam length at 15.2 volts. An optimized s-shape beam is obtained in terms of central plate displacement, up-capacitance, and tuning ratio.

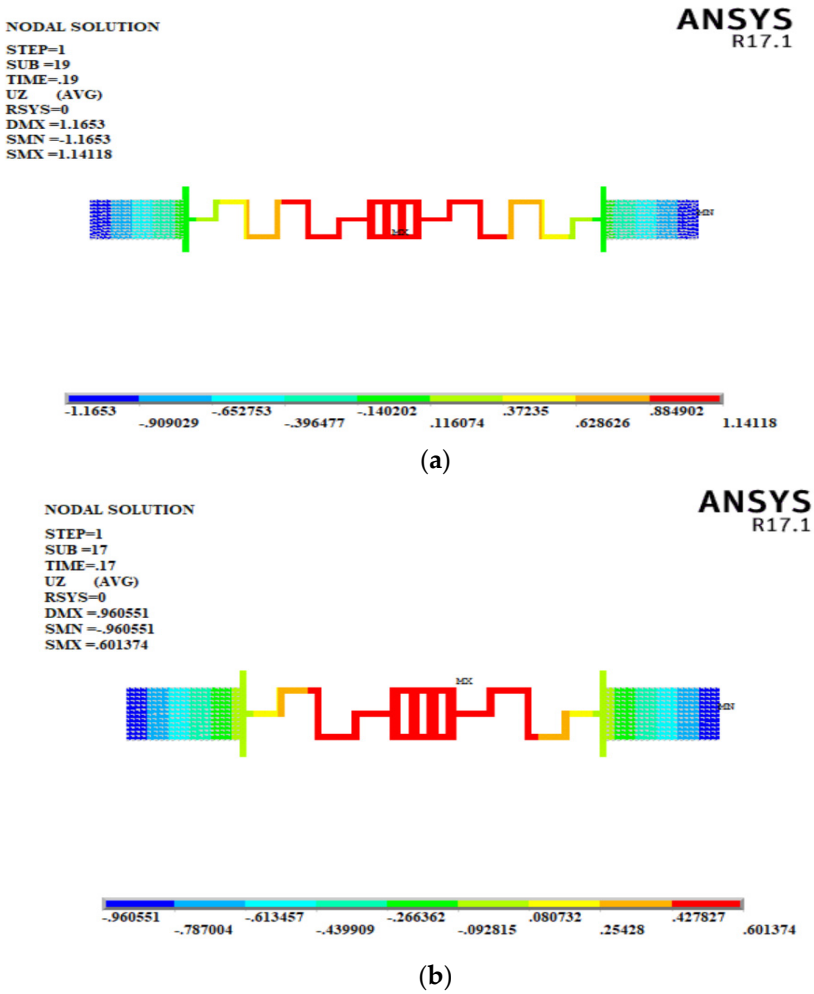

(**a**)

(**b**)

Figure 14. ANSYS APDL results at different lengths of s-shaped beam: (**a**) 290 um; (**b**) 190 um.

3.3.4. Torsion Spring Length Optimization

For the proposed RF MEMS variable capacitor, analysis of the torsion spring length was performed to obtain optimized torsion spring lengths. Varying the length of the torsion spring has a significant effect on the performance of the proposed device. Figure 15 shows the evaluation of capacitor plate displacement and up capacitance at different torsion spring lengths. There is a change in pull-in voltage and displacement by changing the torsion spring length from 30 um to 50 um.

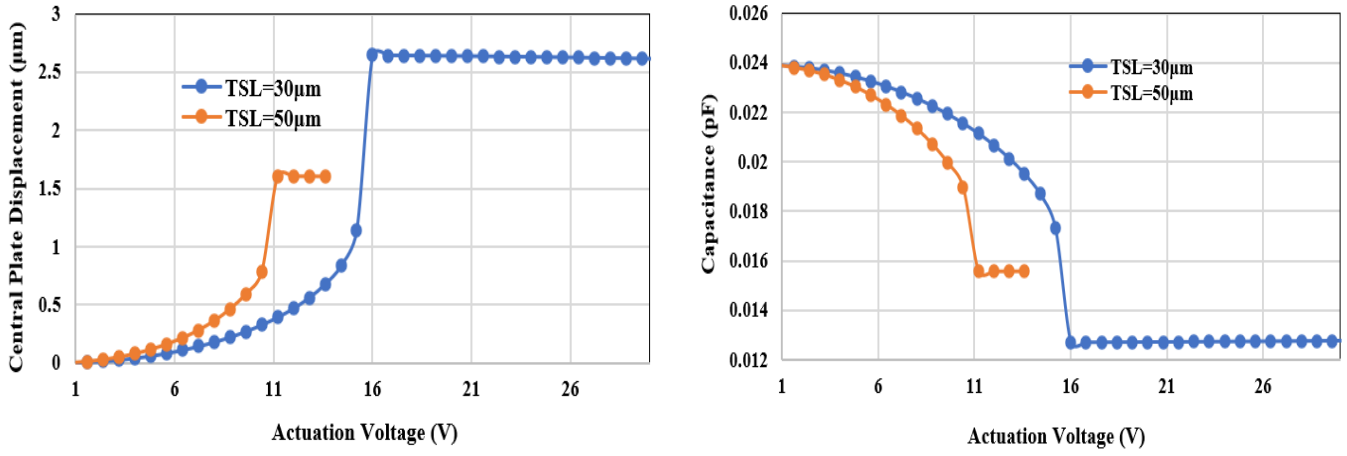

(**a**) (**b**)

Figure 15. Comparison of (**a**) central plate displacement at different torsion spring lengths and (**b**) up-capacitance at different torsion spring lengths.

3.3.5. Varying the Gap between Plates in Capacitor Section

There is a predictable effect on the scattering parameters by varying the gap between the plates within a specific range of frequency (1 GHz to 10 GHz). A parametric analysis of the proposed design is performed to optimize the space between the plates in the capacitor section. From the graph in Figure 16, it is shown that by increasing the gap between the plates, return losses are increased. While there is no difference in insertion loss from varying the gap.

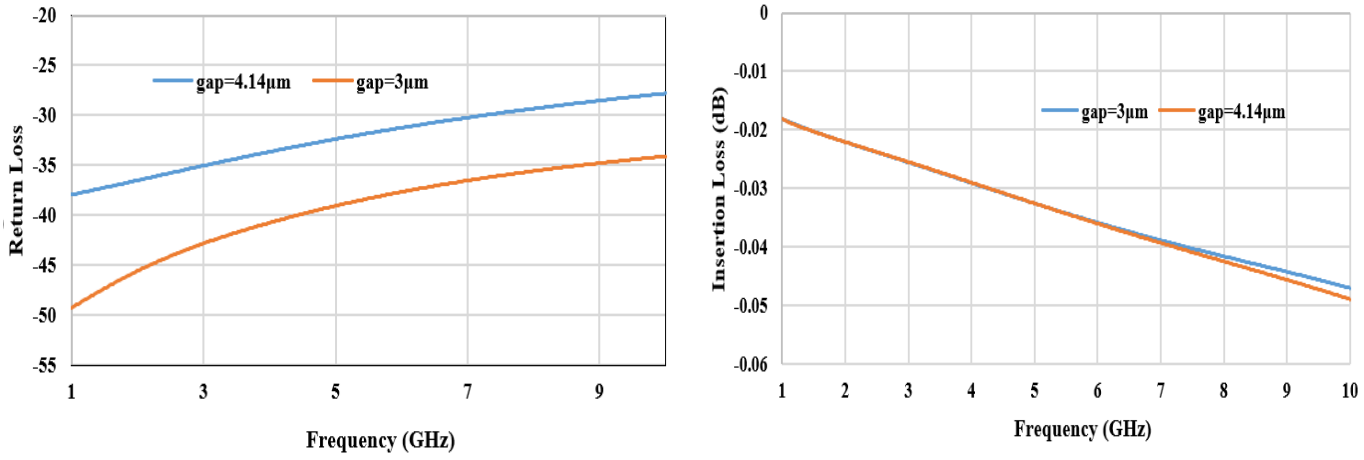

(**a**) (**b**)

Figure 16. Comparison of the (**a**) return loss and (**b**) insertion loss at different gaps between the plates in the capacitor section.

3.3.6. Environmental Effects on the Performance of RF MEMS Variable Capacitor

The reliability of the RF MEMS (radio frequency microelectromechanical system) variable capacitor is influenced by several environmental effects like humidity, temperature variations, contamination, and electrostatic discharge. Its design is optimized in terms of stiction and stress level. Stiction is the main concern, which can be due to variation in humidity and temperature. Slicing the central plate area is one of the approaches used to avoid the stiction problem that leads to better mechanical switching of the device. The contact area is reduced to avoid the stiction issues. Moreover, von Mises stress is optimized to avoid vibration and collapsing issues in the design.

4. Simulation Results with Non-Planar Electrostatic Actuator

Optimization of the proposed RF MEMS variable capacitor with a high linearity factor and large tuning ratio is presented in Section 3. Optimized results are obtained with low actuation voltage.

In this section, an RF MEMS varactor using a non-planar electrostatic actuator is presented. For a non-planar structure of the electrostatic actuator, the length of the top electrode and bottom plates are unequal, as shown in Figure 17. In this case, after applying a voltage to the electrostatic actuator, the top electrode starts moving down due to electrostatic force. The pull-in angle of the actuator plate is mainly dependent on the length of the fixed electrode. Shorter fixed electrode length is used here as compared to the planar structure. So, lower electrode length leads to a maximum pull-in angle, and it allows for the moveable plate to cover the maximum distance in the downward direction. Hence, the actuator plate covers the maximum distance in the downward direction by avoiding the risk of pull-in stability.

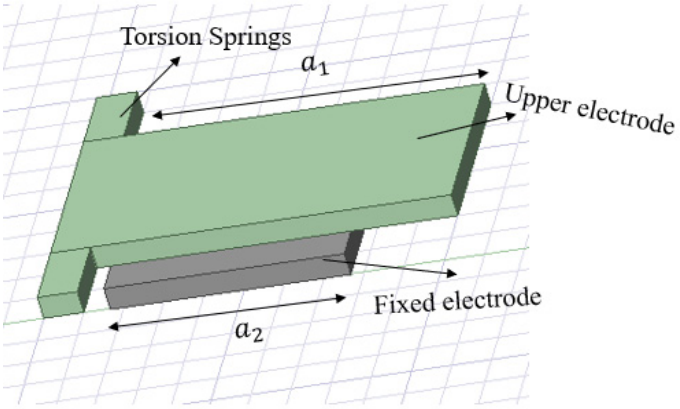

Figure 17. Top view of the non-planar electrostatic actuator.

ANSYS APDL is utilized to obtain a capacitance–voltage response by using a non-planar structure of an electrostatic torsion actuator. Figure 18a,b represents the response of capacitor plate displacement and up capacitance at different actuation voltages. Maximum capacitor plate displacement of 2.022 um is achieved at 47.2 volts by avoiding the pull-in point. The tuning ratio of the proposed varactor is 167%, which is higher as compared to the device by utilizing a planar electrostatic actuator. A non-planar electrostatic actuator is presented to obtain the high tuning ratio by avoiding the pull-in point and allowing for the actuator plate to have maximum travel in the downward direction. Table 3 represents the comparison of the proposed RF MEMS variable capacitor with the literature.

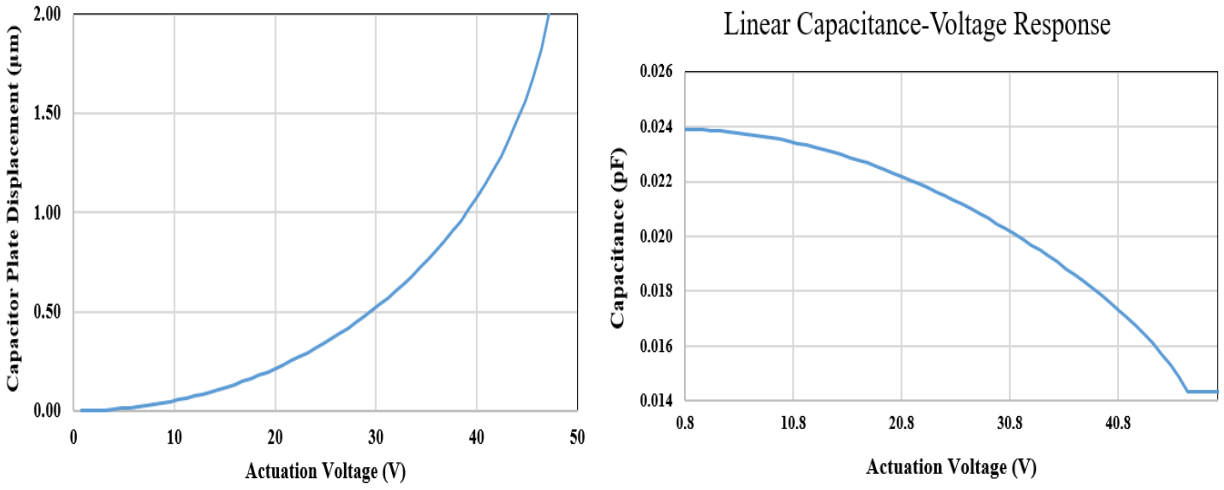

(**a**) (**b**)

Figure 18. Graphical representation of RF-MEMS variable capacitor showing (**a**) central plate displacement and (**b**) central plate capacitance.

Table 3. Comparison of the proposed design with the literature.

Reference	Tuning Rang	Pull-In Limitation	Pull-In Voltage	Linearity Factor	Movement of the Bridge Direction
[13]	134%	Yes	10–45 V	99.5%	Upward direction
[15]	309%	yes	28.24 V	99.92%	Upward direction
[17]	160%	yes	15.2 V	96%	Upward direction
[18]	11×	No	1–100	99.70%	Upward direction
Proposed work	167%	No	47.2	99%	Upward direction

Up-capacitance in the form of pull-in angle can be represented as follows:

$$C_{up\ state} = \frac{\varepsilon A}{d + \alpha_{pull\ in} * l_b} \tag{9}$$

After putting the pull-in angle from Equation (5), capacitance dependence on voltage can be found by the following equation:

$$C_{up\ state} = \frac{\varepsilon A}{d + \frac{-3a_1{a_2}^2\alpha_{max} + \frac{12T_s(a_1\alpha_{max})^3}{\varepsilon w V^2}}{2{a_2}^3} * l_b} \tag{10}$$

To determine the level of linearity of the C–V relationship, a linear factor (*LF*), which is defined as the linear correlation between the capacitance and the voltage response, is introduced [26].

$$LF = \frac{n\sum_{i=1}^{n} C_i V_i - \sum_{i=1}^{n} C_i \sum_{i=1}^{n} V_i}{\sqrt{\left[n\sum_{i=1}^{n} {C_i}^2 - \left(\sum_{i=1}^{n} C_i\right)^2\right]\left[n\sum_{i=1}^{n} {V_i}^2 - \left(\sum_{i=1}^{n} V_i\right)^2\right]}} \tag{11}$$

where n is the number of tests and C_i is the capacitance that correlates with the voltage V_i. The linearity factor (*LF*) is a function of both 0 and 1, and as the curve becomes more straight, it becomes closer to 1. Equation (11) is used to access the linearity factor between capacitance and voltage, which is 99%. Table 4 represents the comparison of the tuning ratio for the MEMS variable capacitor with the planar and non-planar electrostatic actuators.

Table 4. RF MEMS varactor comparison with planar and non-planar electrostatic actuator.

RF MEMS Varactor with Different Actuator Layouts	Length of the Bottom Electrode	Length of the Top Electrode	Pull-In Voltage	Tuning Ratio
Planar electrostatic actuator	150 um	150 um	15.2 V	138%
Non-planar electrostatic actuator	66 um	150 um	47.2 V	167%

5. Conclusions

The proposed study presents the design and modeling of an RF MEMS variable capacitor with an s-shaped beam. This is the first demonstration of an s-shaped beam to be utilized to connect the actuator part and capacitor part. An electrostatic actuator is employed for actuation purposes. Two modes of electrostatic actuators with planar and non-planar structures are proposed to obtain a high tuning ratio for the RF MEMS variable capacitor. Initially, electrical and mechanical analysis of RF MEMS variable capacitor by utilizing the planar structure of the electrostatic actuator is presented at low actuation voltage. The proposed design by introducing the planar structure of the electrostatic actuator shows a 138% tuning ratio at 15.2 V. High linear capacitance–voltage response is achieved for the proposed MEMS variable capacitor. The optimized RF MEMS varactor shows better performance at 5.3 GHz in terms of isolation losses.

For long-term reliability, some of the analyses were carried out in the proposed research design. There are slices in the central plate to avoid stiction issues, which is essential for the switching cycle of the RF MEMS variable capacitor. Optimization of the proposed RF MEMS variable capacitor with a planar electrostatic actuator is performed to obtain high performance with low actuation voltage. Parametric optimization of the proposed design is essential because when the varactor is being fabricated, a parametric investigation of the device is required to study the impact of changing various parameters. Stress analysis is carried out to evaluate the collapsing issues in the device which guarantees that the structure can sustain the applied voltage without collapsing because maximum stress is less than aluminum's yield strength.

Another approach of the electrostatic actuator with non-planar mode is presented. RF MEMS variable capacitor with a non-planar electrostatic actuator operates at high actuation voltage as compared to the RF MEMS variable capacitor with a planar electrostatic actuator. This is because the RF MEMS varactor with the non-planar structure of the actuator allows for the moveable plate to travel long in the downward direction by avoiding the occurrence of pull-in instability. A high linearity factor of 99% is obtained in this case. A tuning ratio of 167% is achieved by preventing the occurrence of pull-in instability. The proposed RF MEMS variable capacitor design has applications in various tunable devices like VCOs and PLL.

Author Contributions: Conceptualization, S.S. and T.A.; methodology, S.S. and T.A.; formal analysis, P.L. and T.A.; simulation, S.S.; validation, T.A. and P.L.; writing—original draft, S.S.; proofreading, T.A.; writing—review and editing, S.S., T.A. and P.L.; supervision, T.A. and P.L.; project administration, T.A. and P.L. All authors have read and agreed to the published version of the manuscript.

Funding: This work is supported by the Higher Education Commission (HEC), Pakistan and the University of Edinburgh, U.K.

Institutional Review Board Statement: Not applicable.

Informed Consent Statement: Not applicable.

Data Availability Statement: Data is available on demand.

Acknowledgments: This work was carried out with support from the Scottish Microelectronics Centre (SMC); the University of Edinburgh, U.K.; and the Higher Education Commission (HEC), Pakistan.

Conflicts of Interest: The authors declare no conflicts of interest.

References

1. Rebeiz, W.G.M. *RF MEMS, Theory, Design and Technology*, 1st ed.; Wiley Interscience: Chichester, UK, 2003; ISBN 978-0-471-20169-4.
2. Rebeiz, G.M.; Entesari, K.; Reines, I.C.; Park, S.J.; El-Tanani, M.A.; Grichener, A.; Brown, A.R. Tuning into RF MEMS. *IEEE Microw. Mag.* **2009**, *10*, 55–72. [CrossRef]
3. De Luis, J.R.; Morris, A.S.; Gu, Q.; De Flaviis, F. A Tunable Asymmetric Notch Filter Using RFMEMS. In Proceedings of the 2010 IEEE MTT-S International Microwave Symposium, Anaheim, CA, USA, 23–28 May 2010.
4. Abbaspour-Tamijani, A.; Laurent, D.; Gabriel, M.R. Miniature and tunable filters using MEMS capacitors. *IEEE Trans. Microw. Theory Tech.* **2003**, *51*, 1878–1885. [CrossRef]
5. Yellepeddi, M.; Mayaram, K. Issues in the Design and Simulation of a MEMS VCO based Phase-Locked Loop. In Proceedings of the 2007 IEEE International Symposium on Circuits and Systems, New Orleans, LA, USA, 27–30 May 2007.
6. Dec, A.; Suyama, K. Microwave MEMS-Based Voltage-Controlled Oscillators. *IEEE Trans. Microw. Theory Tech.* **2000**, *48*, 1943–1949.
7. Khan, F.; Younis, M.I. RF MEMS electrostatically actuated tunable capacitors and their applications: A review. *J. Micromech. Microeng.* **2022**, *32*, 19. [CrossRef]
8. Rebeiz, G.M.; Dussopt, L. *RF MEMS: Theory, Design, and Technology*; John Wiley & Sons: Hoboken, NJ, USA, 2003.
9. Elshurafa, A.; Ho, P.; Salama, K.N. Low voltage RF MEMS variable capacitor with linear C-V response. *Electron. Lett.* **2012**, *48*, 392–393. [CrossRef]
10. Chen, K.; Kovacs, A.; Peroulis, D. Anti-biased RF MEMS Varactor Topology for 20–25 dB Linearity Enhancement. In Proceedings of the 2010 IEEE MTT-S International Microwave Symposium, Anaheim, CA, USA, 23–28 May 2010.
11. Han, C.H.; Choi, D.H.; Yoon, J.B. Parallel-Plate MEMS Variable Capacitor With Superior Linearity and Large Tuning Ratio Using a Levering Structure. *J. Microelectromech. Syst.* **2011**, *20*, 1345–1354. [CrossRef]
12. Han, C.H.; Choi, D.H.; Choi, S.J.; Yoon, J.B. MEMS Variable Capacitor with Superior Linearity and Large Tuning Ratio by Moving the Plate to the Increasing-Gap Direction. In Proceedings of the IEEE 24th International Conference on Micro Electro Mechanical Systems, Cancun, Mexico, 23–27 January 2011.
13. Barrière, F.; Passerieux, D.; Mardivirin, D.; Pothier, A.; Blondy, P. An Inverted-Gap Analog Tuning RF-MEMS Capacitor with 250 milliwatts Power Handling Capability. In Proceedings of the International Conference on Micro Electro Mechanical Systems (MEMS), Paris, France, 29 January–2 February 2012.
14. Shavezipur, M.; Khajepour, A.; Hashemi, S.M. Development of novel segmented-plate linearly tunable MEMS capacitors. *J. Micromech. Microeng.* **2008**, *18*, 035035. [CrossRef]
15. Shavezipur, M.; Khajepour, A.; Hashemi, S.M. A novel linearly tunable butterfly-shape MEMS capacitor. *Microelectron. J.* **2008**, *39*, 756–762. [CrossRef]
16. Shavezipur, M.; Hashemi, S.M.; Khajepour, A.; Nieva, P. Development of a Linearly Tunable Modified Butterfly-Shape. In Proceedings of the ASME International Mechanical Engineering Congress and Exposition, Boston, MA, USA, 31 October–6 November 2008; Volume 2008, pp. 495–500.
17. Shavezipur, M.; Nieva, P.; Khajepour, A.; Hashemi, S.M. Development of parallel-plate-based MEMS tunable capacitors withlinearized capacitance–voltage response and extended tuning range. *J. Micromech. Microeng.* **2009**, *20*, 025009. [CrossRef]
18. Shavezipur, M.; Hashemi, S.M.; Nieva, P.; Khajepour, A. Development of a triangular-plate MEMS tunable capacitor with linear capacitance–voltage response. *Microelectron. Eng.* **2010**, *87*, 1721–1727. [CrossRef]
19. Seok, S.; Choi, W.; Chun, K. A novel linearly tunable MEMS variable capacitor. *J. Micromech. Microeng.* **2001**, *12*, 82–86. [CrossRef]
20. Gong, Z.; Liu, H.; Guo, X.; Liu, Z. Optimization of a MEMS variable capacitor with high linearity and large tuning ratio. *Microsyst. Technol.* **2018**, *24*, 3169–3178. [CrossRef]
21. Roy, A.L.; Bhattacharya, A.; Chaudhuri, R.R.; Bhattacharyya, T.K. Analysis of the Pull-In Phenomenon in Microelectromechanical Varactors. In Proceedings of the 25th International Conference on VLSI Design, Hyderabad, India, 7–11 January 2012.23.
22. Shaheen, S.; Saleem, M.M.; Zaidi, S.M.T. Design and FEM Modeling of an Electrostatic RFMEMS Varactor. In Proceedings of the International Conference on Computing, Electronic and Electrical Engineering, Quetta, Pakistan, 12–13 November 2018.
23. Bensalem, R.; Elsayed, M.Y.; Tawfik, H.H.; Nabki, F.; El-Gamal, M.N. Enhancing Linearity in Parallel-Plate MEMS Varactors through Repulsive Actuation. *Micro* **2023**, *3*, 811–821. [CrossRef]
24. Degani, O.; Socher, E.; Lipson, A.; Leitner, T.; Setter, D.J.; Kaldor, S.; Nemirovsky, Y. Pull-in study of an electrostatic torsion microactuator. *J. Microelectromech. Syst.* **1998**, *7*, 373–379. [CrossRef]
25. Rebeiz, G.M. *RF Mems-Theory, Design and Technology*; Wiley: New York, NY, USA, 2003; Volume 53. [CrossRef]
26. Weisstein, E.W. Math World, Correlation Coefficient. 2006. A Wolfram Web Resource. Available online: http://mathworld.wolfram.com/CorrelationCoefficient.html (accessed on 27 June 2024).